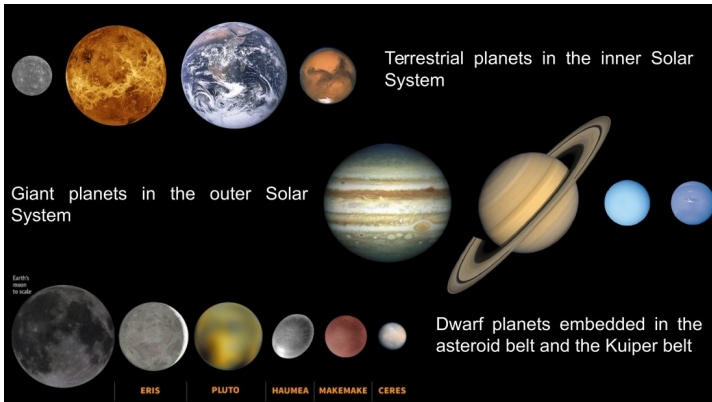


The Solar System

In this chapter the physical and dynamical properties of the Solar System are briefly illustrated. They are also interpreted in light of the standard model of planet formation. Let's start by listing the bodies populating the solar system.

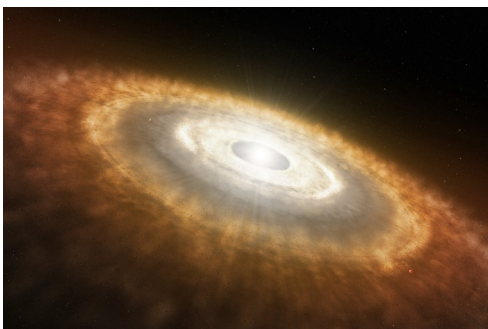


There are 8 planets and some dwarf planets like Pluto, Ceres (a former asteroid), Sedna, Haumeamea (in the Kuiper Belt). Most planets have Moons with a mass ratio ranging from 0.117 (the Pluto-Charon system), 0.0123 (the Moon-Earth system) down to smaller values.

The solar system is also populated by minor bodies called asteroids and comets which are believed to be the remnant of the building blocks of planets, the planetesimals.



Finally, the space among planets, asteroids and comets is populated by dust particles, byproducts of collisions between minor bodies. They distribute as rings surrounding the sun, a debris disk. The lifetime of dust grains is limited since they spiral towards the sun so the dust population needs to be replenished by ongoing collisions in the asteroid and Kuiper belts.



In Table 1 the most relevant dynamical and physical properties of the planets are summarized. It is noteworthy that there is a correlation between the heliocentric distance of the planet and its density. Terrestrial planets (Mercury, Venus, Earth and Mars) are within 1.5 au from the sun and their

Object	Orbital Semimajor Axis (AU)	Orbital Period (Earth Years)	Mass (Earth Masses)	Radius (Earth Radii)	Number of Known Satellites	Rotation Period * (days)	Average Density (kg/m ³) (g/cm ³)	
Mercury	0.39	0.24	0.055	0.38	0	59	5400	5.4
Venus	0.72	0.62	0.82	0.95	0	-243	5200	5.2
Earth	1.0	1.0	1.0	1.0	1	1.0	5500	5.5
Moon	—	—	0.012	0.27	—	27.3	3300	3.3
Mars	1.52	1.9	0.11	0.53	2	1.0	3900	3.9
Ceres (asteroid)	2.8	4.7	0.00015	0.073	0	0.38	2700	2.7
Jupiter	5.2	11.9	318	11.2	63	0.41	1300	1.3
Saturn	9.5	29.4	95	9.5	56	0.44	700	0.7
Uranus	19.2	84	15	4.0	27	-0.72	1300	1.3
Neptune	30.1	164	17	3.9	13	0.67	1600	1.6
Pluto (Kuiper belt object)	39.5	248	0.002	0.2	3	-6.4	2100	2.1
Hale-Bopp (comet)	180	2400	1.0×10^{-9}	0.004	—	0.47	100	0.1
Sun	—	—	332,000	109	—	25.8	1400	1.4

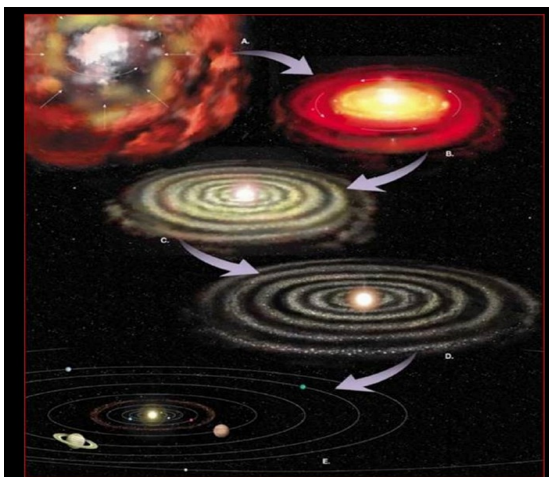
**A negative rotation period indicates retrograde (backward) rotation relative to the sense in which all planets orbit the Sun.*

Copyright © 2008 Pearson Education, Inc., publishing as Pearson Addison-Wesley.

densities are high, while giant planets (Jupiter, Saturn, Uranus and Neptune) are orbiting beyond 5 au and have on average low densities. This correlation must be related to the formation mechanism.

The standard model of planet formation

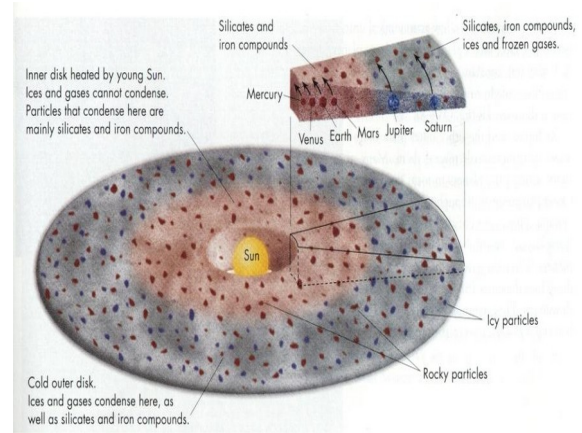
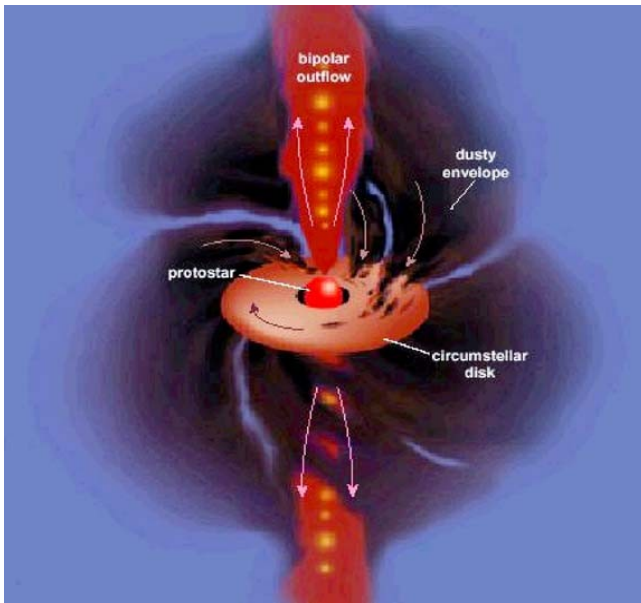
The planet formation model developed to explain the solar system properties, called the “standard model”, consists of 6 main steps:



- 1) A protostellar cloud or part of it collapses into a protostar
- 2) A circumstellar disk forms around the protostar
- 3) Pebbles and planetesimals grow from the dust populating the circumstellar disk
- 4) Planetesimal and pebbles accumulate into planetary embryos
- 5) Terrestrial planets and the core of giant planets grow from collisions between planetary embryos and leftover pebbles and planetesimals
- 6) Infall of gas on the core of giant planets like Jupiter and Saturn.

The cradle of planets: circumstellar disks.

A disk of rotating circumstellar material usually form around a growing protostar as a consequence of angular momentum conservation during cloud collapse. The initial stages of the disk are quite turbulent due to infall of gas and dust on the disk. This period is followed by a more quiet state



during which the dust settles towards the middle plane of the disk. A temperature gradient is present with higher temperatures in the inner regions of the disk. The so called

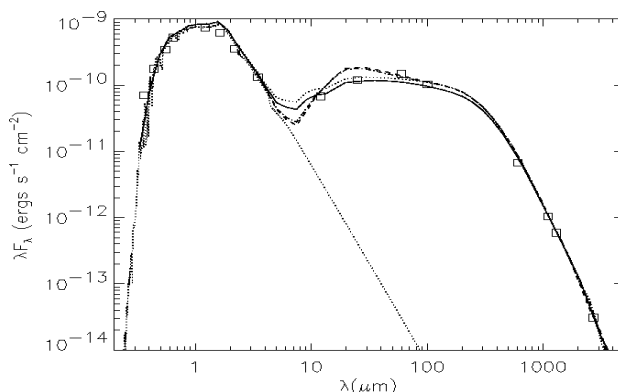
“snow line” or “frost line” marks the radial distance at which the disk teperature drops below the condensation temperature of a particular ice (H_2O , CO_2 , NH_3). For exmple, the “frost line” of water ice is located around 3-5 au for circumstellar disks around solar type stars.

Circumstellar disks around stars can be detected with different methods:

- 1) Infrared excess in the power spectrum of the star
- 2) Direct imaging with high resolution instruments (HST, ALMA, SPHERE...)

Infrared excess and information it brings

If a circumstellar disk is present around a star, the dust present in the disk emits at a lower temperature respect to the star and the blackbody radiation falls within the infrared spectral range. As a consequence, the spectrum of the star appears like the combination of a blackbody with a superficial temperature of about 6000 K (for solar-like stars) and that of a colder source (the disk) with a temperature below 1000 K, the infrared excess.



In figure it is shown the spectrum of a star surrounded by a disk whose presence is deduced by the additional infrared emission. The different shapes of the infrared emission can give insights on the disk evolution.

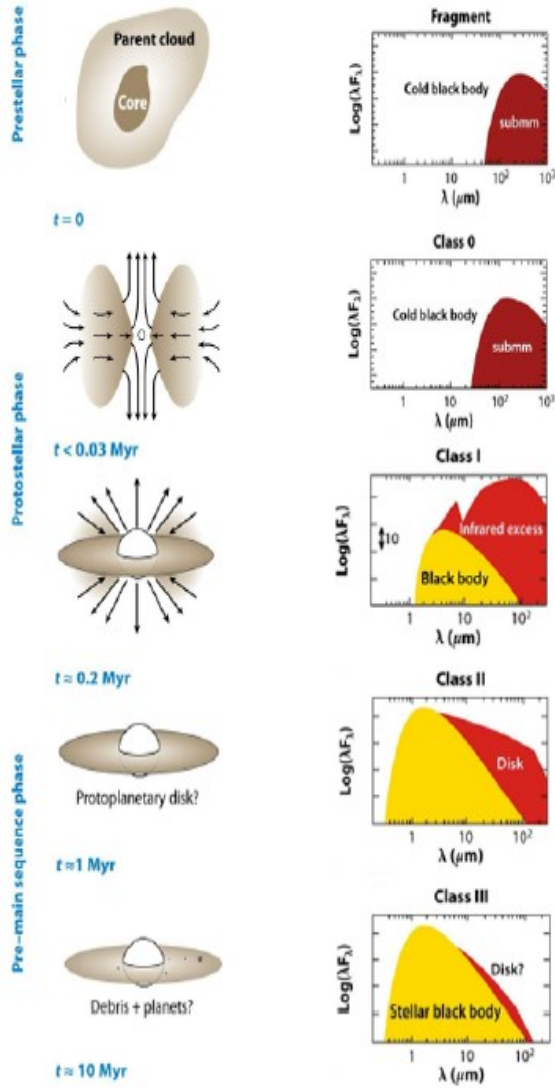
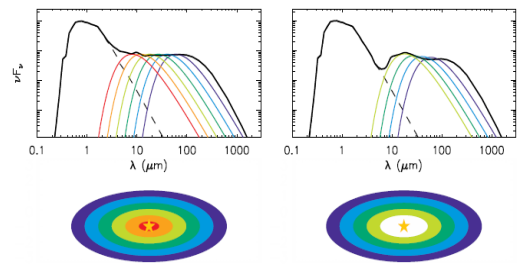


Figure 1.1: Cartoon image illustrating the star and formation process (left) with the expected SEDs (right). A dense molecular cloud collapses under its own gravity and, due to its initial rotation, forms a disc which carries most of the angular momentum of the primordial nebula and slowly accretes onto the central star. Image adapted from André (2002).

In this figure the different shapes of the infrared excess are illustrated at different evolutionary times of the circumstellar disk, from the formation of the protostar, whose spectrum is shown in yellow, down to the final stages when only a debris is still present. A debris disk is not always present and for an evolved star the infrared excess may be totally absent. It is interesting to note that the infrared excess allows also to identify the so called “transition disks”, circumstellar disks in an advanced stage of evolution where the central region of the disk is empty. This hole in the gas and dust density appears as a gap in the spectrum, as illustrated in the figure here below.



From the shape of the infrared excess it is also possible to derive approximate profiles for the superficial gas density distribution and temperature. A power law is usually adopted for both the superficial gas density and temperature.

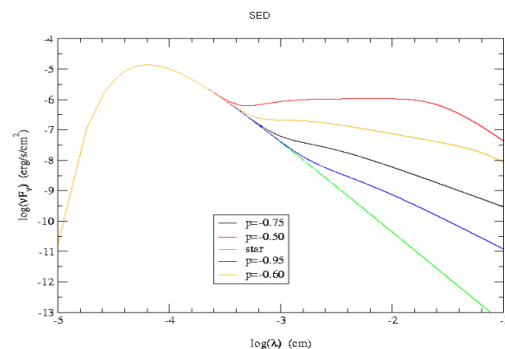
$$\Sigma = \Sigma_0 \left(\frac{R}{R_0} \right)^q \quad \Sigma_0 \approx 10^2 - 10^4 \text{ g/cm}^2$$

$$T(R) = T_0 \left(\frac{R}{R_0} \right)^p \quad T_0 \approx 1000 - 2000 \text{ K}$$

By fitting the infrared excess it is possible to derive approximate values for Σ_0 , T_0 , q , p . A typical reference disk is the so called Minimum Mass Solar Nebula

$$\Sigma = 1700 \frac{\text{g}}{\text{cm}^2} \left(\frac{R}{1 \text{ au}} \right)^{-3/2} \quad \text{giving a total mass in the disk of } M_d \sim 0.01 M_{\text{sun}} \text{ whose profile is}$$

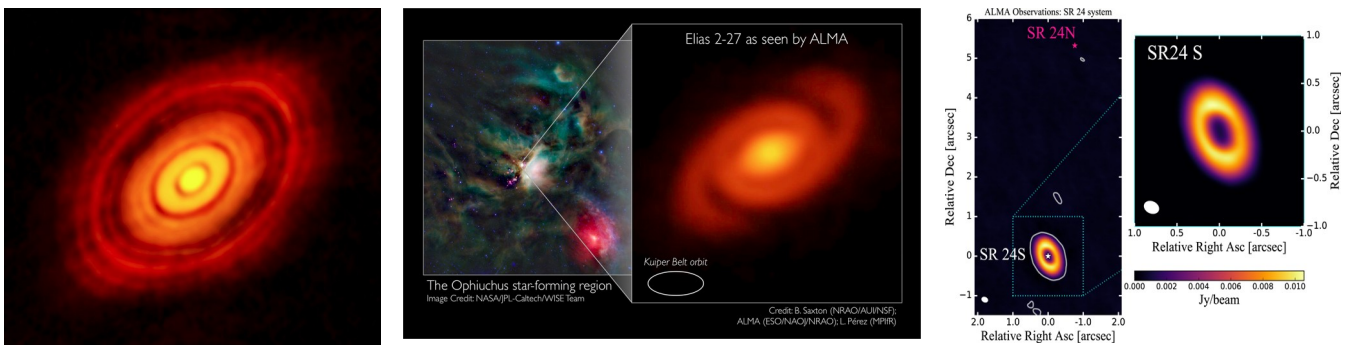
obtained by smearing the mass of the planets on a disk extending approximately for 40 au and



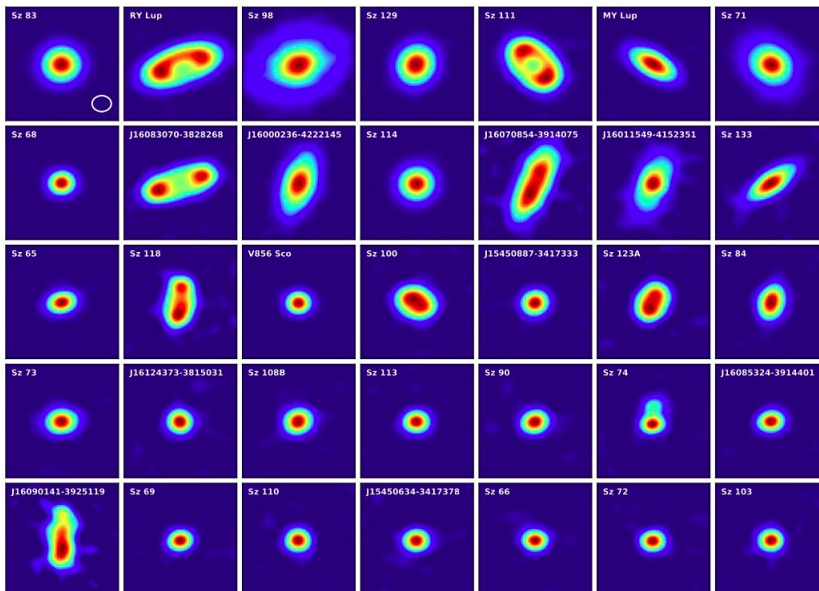
reconstructing the gas density assuming a dust-to-gas ratio of 0.01 (the classical interstellar value). Recently, on the basis of extrasolar planetary systems, in particular those with packed close to the star planets, more massive disks are assumed (Minimum Mass Extrasolar Nebula, MMEN) with a values of Σ_0 5 to 20 times higher than the MMSN.

The circumstellar disk zoo.

With the arrival of ALMA (Atacama Large Millimeter Array) high resolution images have become possible. They highlight many different features in disks like gaps as in the first disk to be imaged around HL Tau, spiral waves, inner holes, different distribution between dust and gas.

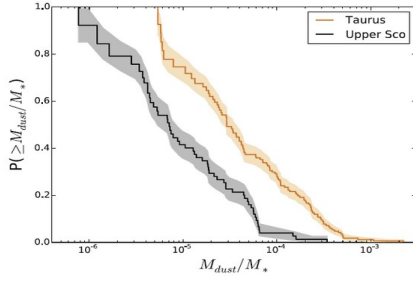


Thanks to the capability of ALMA it has been possible to image a large sample of disk within different stellar clusters and star forming regions obtaining statistical estimates of the fraction of stars with disk and of their lifetime. One example is shown in the bottom figure showing a sample of disks in the Lupus low mass star forming region with an age of 1~2 Myr.



Younger regions are expected to have more massive disks since disks loose mass because of viscous evolution and photoevaporation. This is confirmed by comparing star forming regions of different ages (the star in the region have approximately the same age). In the figure below, taken from Barenfeld et al. (2016) the younger Taurus region (age ~ 1-2 Myr) is compared to the older Upper Scorpius OB Association (age ~ 5-11 Myr). A cumulative distribution of the disks in each region with mass larger than a

given M_{dust}/M_{star} ratio is computed from observations. The average mass of disks in the older region is significantly lower than that in the younger region.



Circumstellar disk evolution

1) Viscous evolution

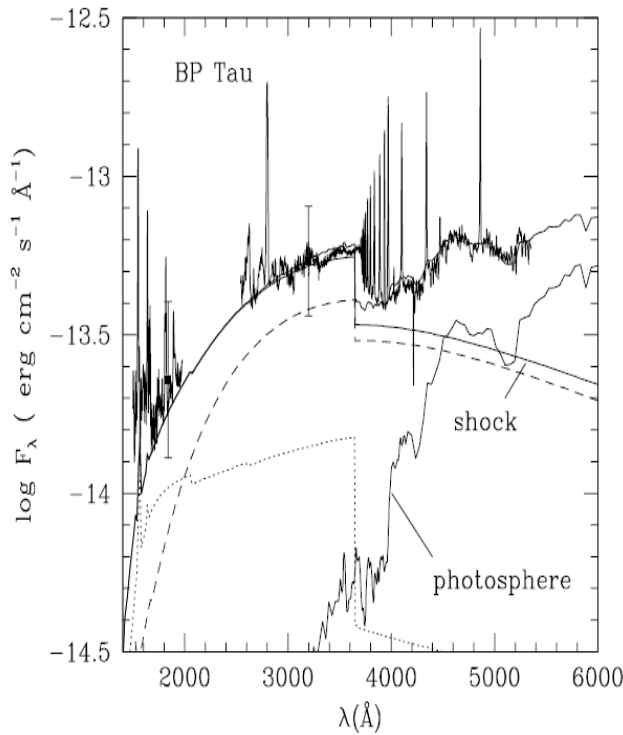
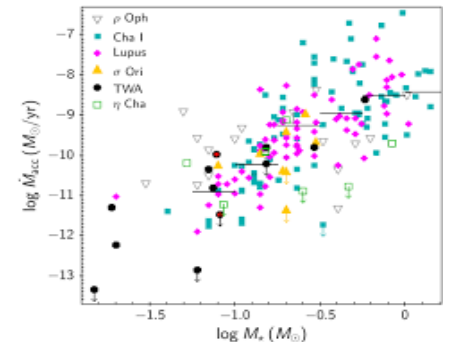


FIG. 1.—Comparison between observed fluxes and shock-model emission for BP Tau. Observations (*thick solid line*) are optical spectrum from GHBC, mean fluxes, and LW and SW *IUE* fluxes, defined by eq. (2). *IUE* fluxes have been smoothed by 5 pixels for better visualization. The mean flux level at 2700 and 1800 Å and range of variability are indicated by the squares and error bars. The theoretical model (*thin solid line*) is composed of the emission from the shock and from the stellar photosphere. The shock emission, in turn, is the sum of the emission from attenuated post-shock and diffuse preshock (*dotted line*) and the heated atmosphere (*dashed line*) (Paper I). The shock parameters used are $\log \mathcal{F} = 11.5$, $f = 0.007$, and $A_V = 0.51$.

Observations of an ultraviolet and optical excess in the spectrum of a star show that there is mass accretion on the star surface due to disk mass infall. This is illustrated in the figure where the photospheric emission at small wavelength (the bottom solid line) is overcome by the emission by the shock wave produced by disk material impacting the surface of the star. The upper solid line is the combination of shock and photospheric emission which is close to the observed spectrum of the star. There is a strong correlation between the mass of the star and the disk accretion rate given by the equation

$$\log(\dot{M}_{acc}) = -7.9 + 2.1 \log(M_{star})$$

given in Hartmann et al. (2016). The mass accretion on the star is driven by the viscosity of the disk causing a transfer of angular momentum toward the outer regions. The accretion rate covers a wide range of values ranging from $10^{-12} M_{sun}/yr$ to $10^{-7} M_{sun}/yr$ for more massive stars, as shown in the bottom figure



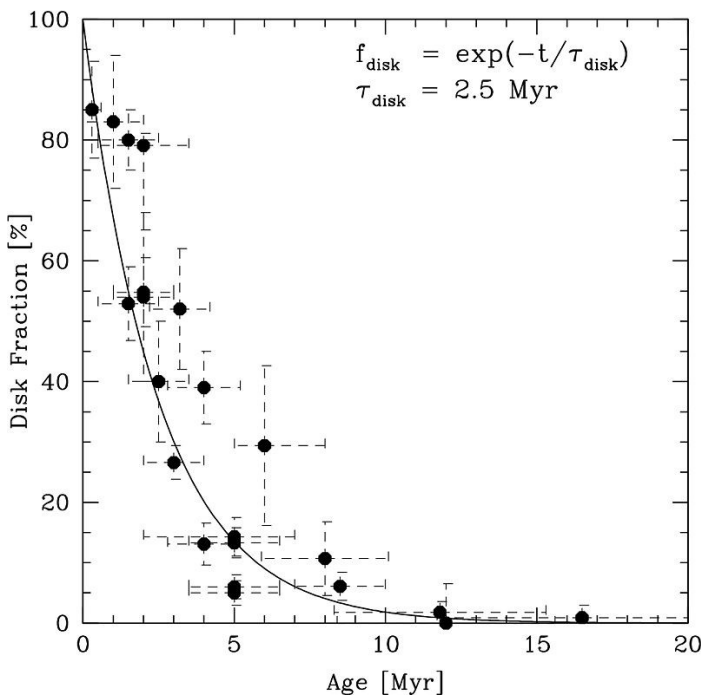
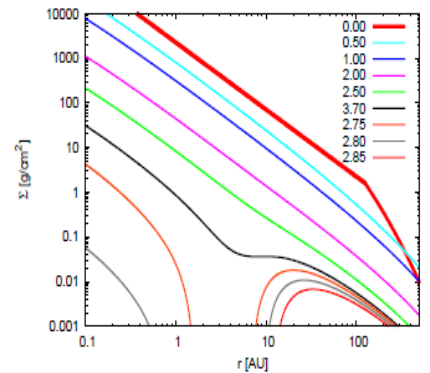
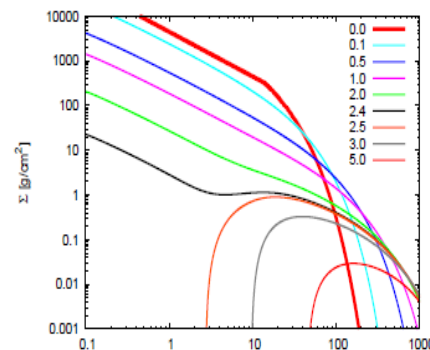
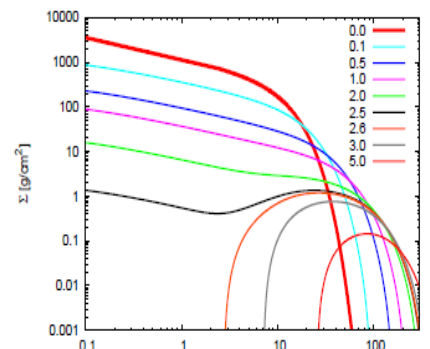
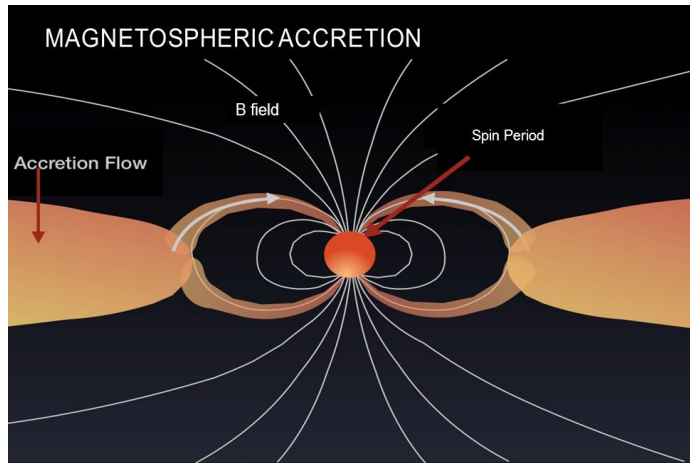
The material of the inner border of the disk is ionised by the star radiation and it impacts the star surface following the magnetic dipolar field lines. Temperatures of the order of 10^4 K are reached at the impact region.

The long term evolution of a disk is determined by its viscous evolution, by photoevaporation and by planet formation. A bidimensional equation can be solved to find the superficial density evolution of the gas in the disk, which is

$$\frac{\partial \Sigma}{\partial t} - \frac{3}{r} \frac{\partial}{\partial r} \left(r^{1/2} \frac{\partial}{\partial r} (\Sigma \nu) \right) = -\dot{\Sigma}_{PE}$$

where $\dot{\Sigma}_{PE}$ is the mass loss due to gas photoevaporation driven by X and EUV and FUV ultraviolet radiation from the star. Solving the equation leads to the following curves (D'angelo and Marzari, 2012). The different colors refer to progressively longer evolution time up to 5 Myr. In most cases, an inner hole forms at the center of the disk, as observed in transition disks.

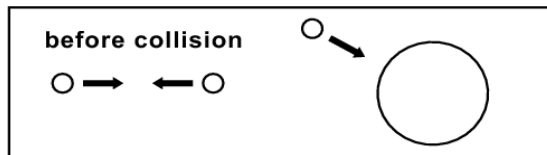
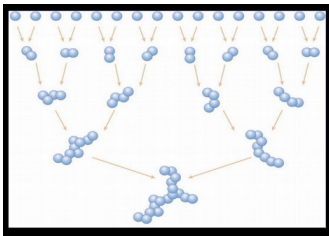
These theoretical calculations also predict that the lifetime of a circumstellar disk is around 3-5 Myr. This is also confirmed by observations of the fraction of stars retaining a disk in stellar clusters of different ages. As shown in the bottom figure (Mamajek 2009) the fraction of stars with disks after 10 Myr is very small.



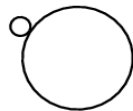
The long lasting problem of planetesimal formation.

During the quiet phase of the disk, the dust settles towards the middle plane of the disk and it grows into larger bodies. However, there is a theoretical transition from dust particles to planetesimals when the drag of the gas becomes a perturbation respect to the dominant Keplerian motion. This typically occurs at sizes of the order of 10 km in diameter. For smaller sizes the evolution is dominated by the gas and the motion is not keplerian in the sense that when a particle moves around the star, it does not cross the median plane of the disk but is 'suspended' in the gas. On the other side, when the bodies are in the planetesimal range, they perform a keplerian orbit which has a given inclination and the body crosses at the nodal line the median plane of the disk. Of course, a sharp cut in size is not possible and there will be a slow transition from one kind of motion to the other depending on the size of the body. Why a planetesimal theory? Because at present in the solar system there are still some of these planetesimals which did not have a chance to growth into a full planet, i.e. asteroids and comets which come with a large variety of sizes.

At present, the most intriguing problem is how planetesimals formed and what was their initial size and size distribution. It was believed that the progressive accumulation of dust into larger bodies lead directly to planetesimals as shown in the figure via two-body collisions.



S1 (*hit & stick*)



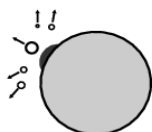
S2 (*sticking through surface effects*)



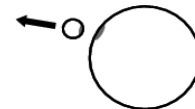
S3 (*sticking by penetration*)



S4 (*mass transfer*)



B1 (*bouncing with compaction*)



B2 (*bouncing with mass transfer*)



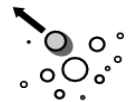
F1 (*fragmentation*)



F2 (*erosion*)



F3 (*fragmentation with mass transfer*)



However, the outcome of collisions strongly depends on the mutual impact velocity. If it is too high, fragmentation and cratering with mass loss dominate and the dust accumulation process is halted. The relative velocity between dust particles is determined by the following contribution:

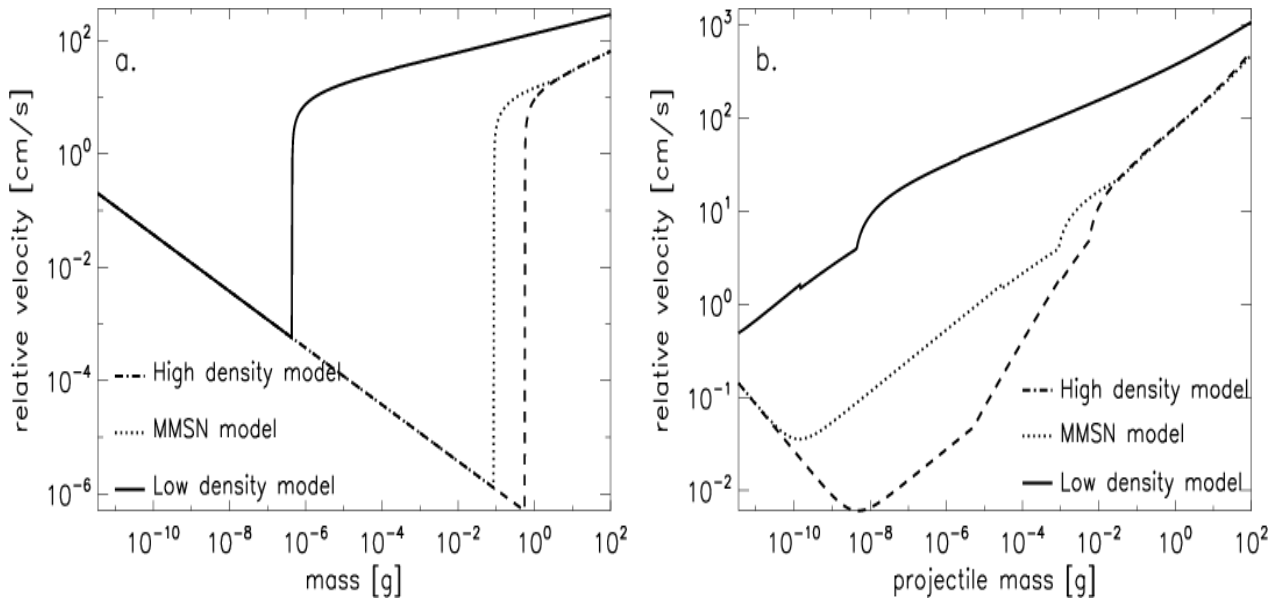
1) Brownian motion : $v \sim v_{th} = \sqrt{\frac{8 K_B T}{\pi \mu m_H}}$

2) Differential vertical settling $v_{settle} = \frac{\rho_d}{\rho_g} \frac{s}{v_{th}} \Omega^2 z$

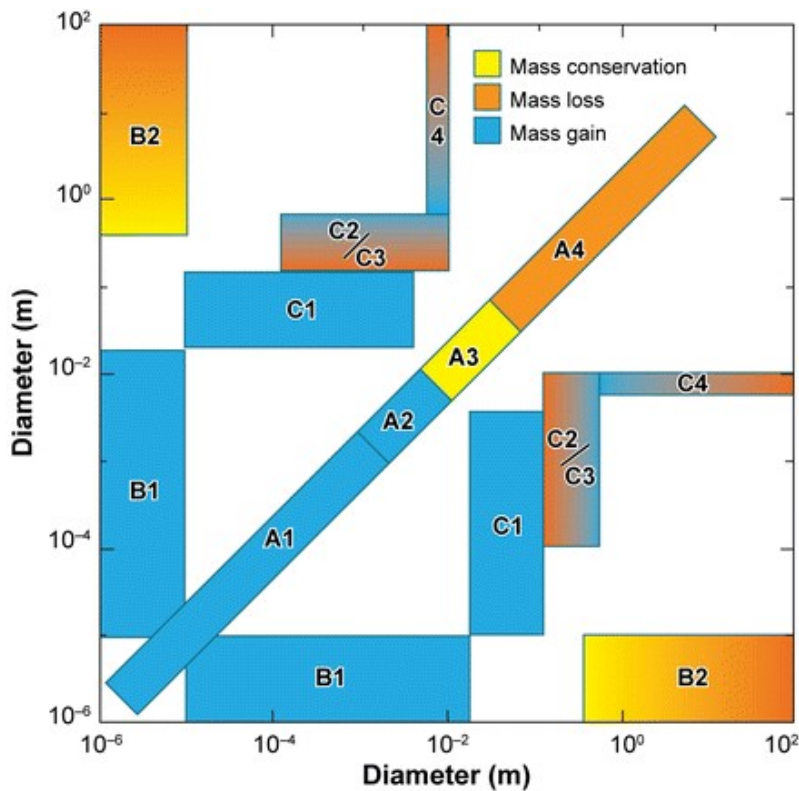
3) Differential radial drift $v_{radial} = -\eta \frac{\rho_d}{\rho_g} \frac{s}{v_{th}} \Omega^2 R$

4) Turbulence ??

Combining all contributions, the estimated relative velocities are approximately those reported in the bottom figures (Zsom et al. 2010). The figure on the left is for impacts between equal size dust particles while that on the right for particles with a 1/100 in diameter.



Laboratory experiments with these impact velocities have shown that accretion is possible only up to bodies 1-10 cm in size, the so called pebbles.



The figure on the left shows the diameters for which, given the above impact velocity distributions, accretion is possible (blue areas) and, on the contrary, mass loss occurs during collisions (orange areas). For diameters larger than some centimeters accretion into larger bodies appears difficult if not impossible. There are factors which may enhance the sticking between dust particles like 1) dipole charging which may lead to electrostatic attraction 2) aerodynamical reaccretion, since smaller fragments of a collision feel a stronger gas wind and are accreted back 3) magnetic sticking 4) compositional features which may enhance the sticking.

 Blum J, Wurm G. 2008. *Annu. Rev. Astron. Astrophys.* 46:21–56

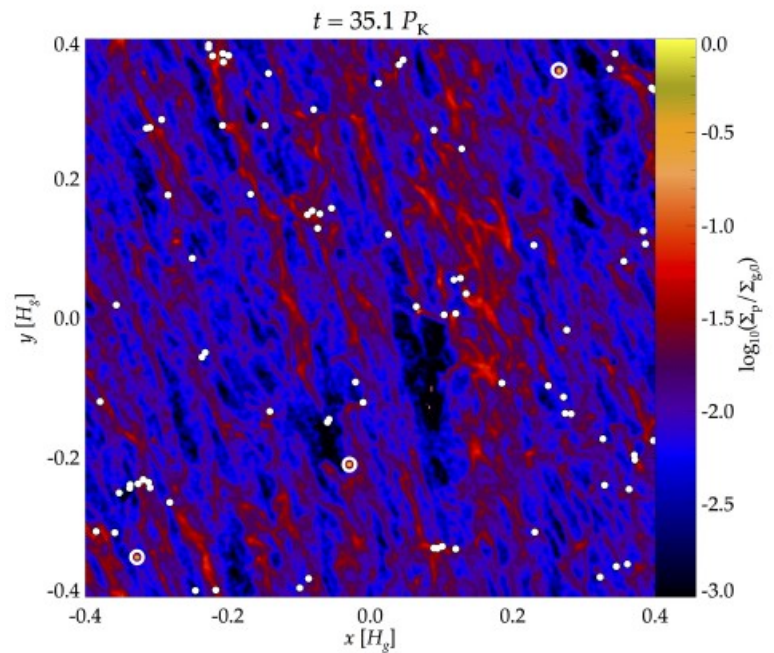
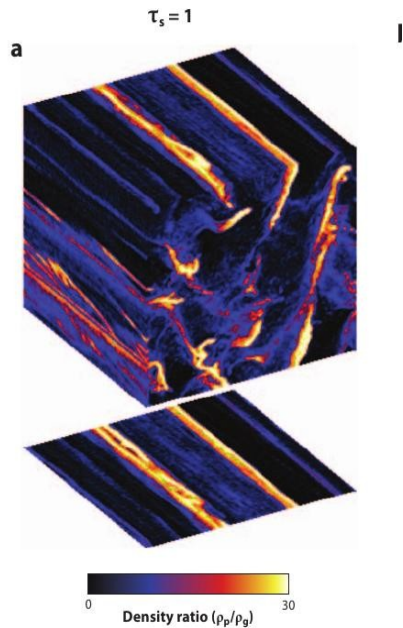
An additional negative factor for direct accumulation of dust into planetesimals is the “meter barrier” when rapid migration of boulder-sized solids (~ 10 - 100 cm) occurs. The interaction with

the gas component of the disk leads to a fast spiraling of bodies about 1 m in size, although notable drift will begin in the mm to cm-size regime. The inward radial velocity becomes comparable to the Keplerian velocity $v_{radial} = -0.5 \eta V_K$ and the timescale to drift towards the star can be of the order of 100-1000 yr. This may prevent further growth of dust into planetesimals.

Alternative paths to planetesimal formation

In alternative to the continuous growth of dust directly into planetesimals, formation models based on a strong interaction with the gas have been proposed. The first assumes that the dust settles in the middle plane of the disk where gravitational instability occurs leading to the direct formation of planetesimals. However, this model does not take into account of the Kelvin – Helmholtz instability due to the backreaction of dust on the gas. This creates turbulence that diffuses the dust particles reducing the density below the value needed for gravitational instability to be effective. An intense photoevaporation may reduce the gas density allowing the gravitational instability to occur anyway, but this seems unlikely in the initial phases of evolution of a disk.

A different kind of instability, the “streaming instability”, may lead to the clumping of a large number of dust particles into planetesimals. Starting from pebbles, planetesimals as large as 100 km and bigger can be directly formed via this kind of instability. Numerical models based on the pencil code, a code cutting a small cube within the disk and following the evolution of dust and gas, show that the instability leads to the formation of high density filaments in the gas which trap the dust and form fluffy planetesimals.



Even this theory for spontaneous planetesimal formation by particle condensation (Johansen and Youdin 2007) requires a high dust density in the middle plane of the disk (~ 1 dust-to-gas mass ratio). This model appears to explain also the occurrence of a large number of equal-sized binaries in the Kuiper belt (Nesvorny et al, 2019). It is interesting to note that ANY KIND of instability may lead to the formation of planetesimals as far as it produces pressure bumps where the dust is trapped. Vertical shear instability, related to the different rotation velocity of gas at different z -values, baroclinic instability, gravitational instability etc. can lead to the formation of dust traps (pressure bumps) where the dust can clump. Maybe, the knowledge of the initial size distribution of planetesimals might help to discriminate among these alternative source of instability.

There are also other mechanisms capable of trapping dust particles into a restricted volume which may trigger the gravitational instability needed to form planetesimals.

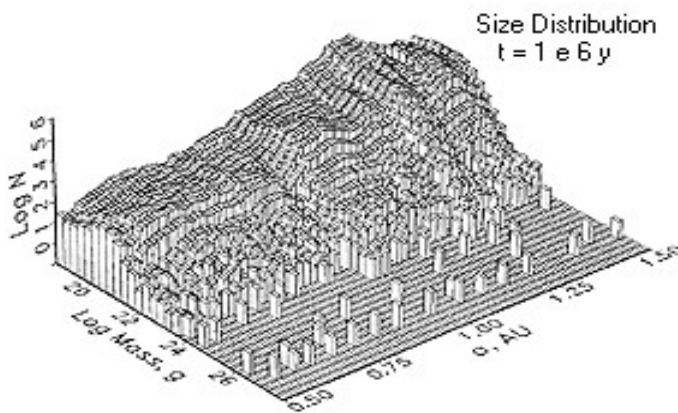
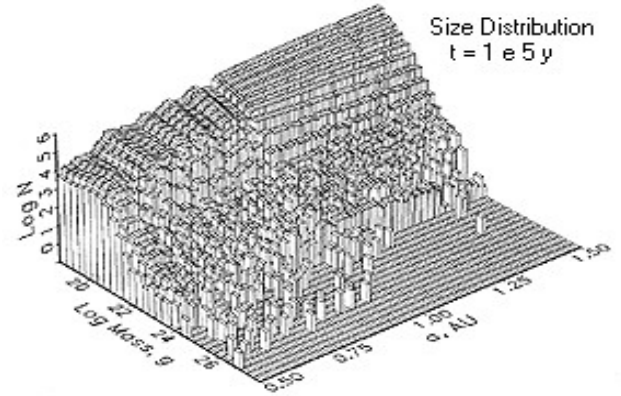
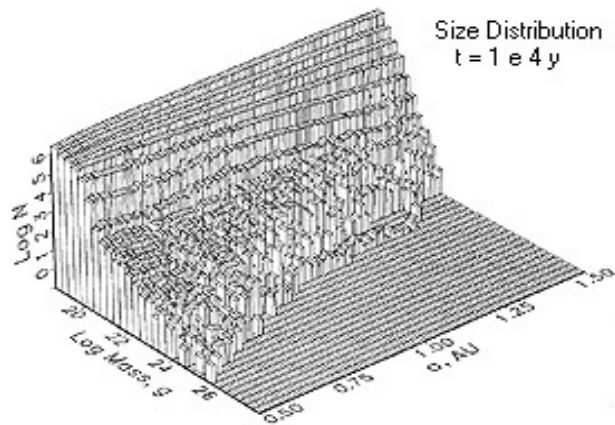
- 1) If Magneto Rotational Instability (MRI) is responsible for the viscosity in disks, at the border of a dead zone, where the ionization is too low to allow the onset of a significant viscosity, a gas bump forma trapping dust (Dzyurkevich et al. 2019).
- 2) Giant planets produce a gap in the gas. At the edge of these gaps dust cumulates because of the pressure bump and can favor clumping (Pinilla et al. 2012).
- 3) Near a frost line, large grains coming from outside may shrink due to evaporation. This would cause a slow down of the inward drift velocity leading to a higher dust density (Drazkowska and Alibert, 2017).

An interesting paper on planetesimal formation is Blum, Space Science Review 2018.

Planetesimal accretion

The planetesimal accretion process can be divided in 3 different stages:

- 1) Runaway growth: some planetesimal outrun the others and grow at a faster pace detaching from the other planetesimals



The runaway growth is shown in these figures where an initial population of planetesimals located around 1 au is evolved via mutual collisions (planet building numerical model), After about 1 Myr a large fraction of the initial mass is in a few bodies more massive than the remnant population.

2) Transition to oligarchic growth occurs when the runaway embryos become massive enough to affect planetesimals' random velocities and, as a consequence, the growth regime switches to a slower one (typically when the mass of the embryo exceeds 100 times the average mass of planetesimals). The runaway embryos excite the eccentricities and inclinations of the planetesimals and the growth rate of the protoplanets decrease as a consequence of the greater relative velocities between the protoplanet and planetesimals. However, the mass ratio of the protoplanet and planetesimals continues to increase with time. The protoplanets keeping a typical orbital separation of 10 Hill's radius, where the Hill's radius is defined as:

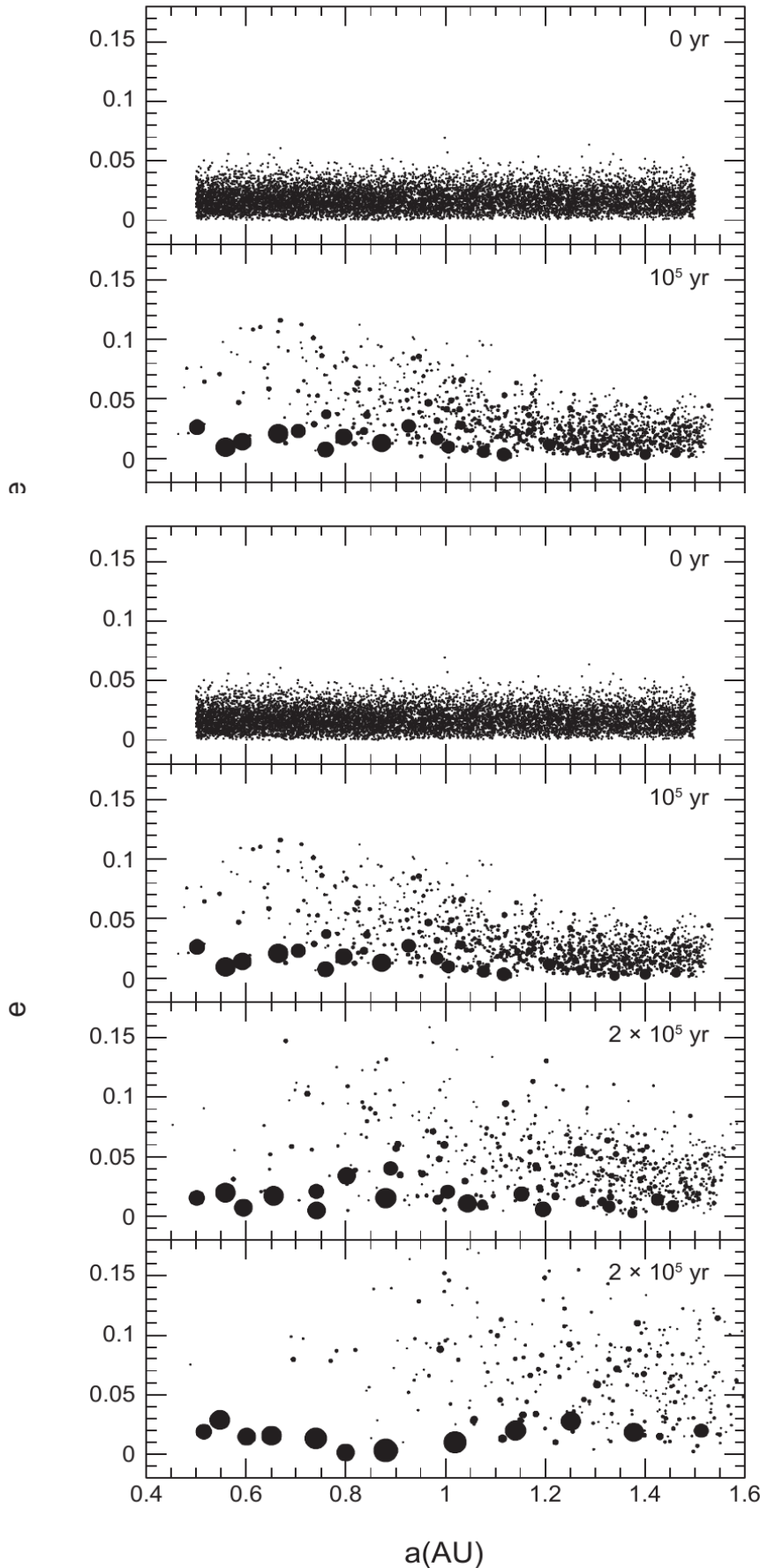
$$R_H = \left(\frac{m}{3M_s} \right)^{1/3} a$$

where m is the mass of the protoplanet, M_s the mass of the star and a the semi-major axis of the protoplanet. Thus, protoplanets grow "oligarchically" and no substantial accretion between the remaining planetesimals occurs. The mass distribution becomes bi-modal: a small number of protoplanetary embryos and a large number of small planetesimals (Kokubo & Ida, 1998) and these several protoplanets dominate the planetesimal system. The oligarchic growth phase yields a disk with Moon-to-Mars-sized objects embedded in a swarm of smaller bodies. The end up dynamically isolated i.e. they do not further grow at a mass value equal to

$$m_{iso} = 0.16 \left(f_{ice} \frac{\Sigma_0}{10} \right)^{3/2} \left(\frac{a}{1 \text{ au}} \right)^{3/2(2-p)} M_{Earth} \left(\frac{b}{10 \cdot r_H} \right)^{3/2}$$

where b is the orbital separation of embryos,

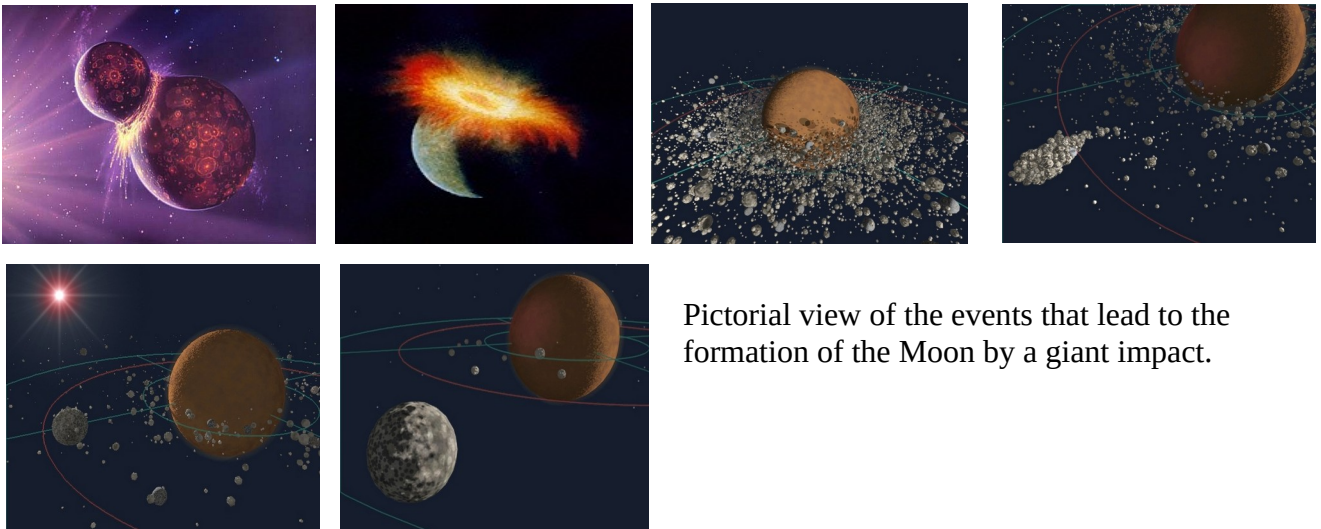
Σ_0 is the dust density of the circumstellar disk at 1 au and f_{ice} is the fraction of icy solid material respect to the standard dust surface density ($f_{ice} \sim 2-4$).



In the figure an example of oligarchic growth computed via an N-body numerical simulation is shown (Kokubo & Ida, 2002). Initially, the bodies have a mass of $2.5 \cdot 10^{-4} M_{Earth}$ and they grow by mutual collisions.

3) The giant impact stage.

When there is insufficient damping of protoplanet eccentricity by dynamical friction of smaller planetesimals (Kenyon & Bromley, 2006) via repeated close encounters, the “oligarchs” excite each other orbits. The evolution becomes chaotic, they have frequent close encounters and giant embryo-embryo collisions occur with the formation of larger bodies like Earth and Venus. Mars could be the remnant of a protoplanet while Mercury with its large iron-rich core (about 70% of its mass) could have survived an impact with a larger body that stripped of its mantle in a high velocity collision in a hit-and-run scenario (Asphaug & Reufer, 2014). This is slightly different from the standard giant impact model for Moon formation (Canup, 2004) since in this case the Earth captures the fragments of the smaller body that impacted it and the material, excavated from Earth and from the projectile, form a ring around the planet from which the Moon formed.



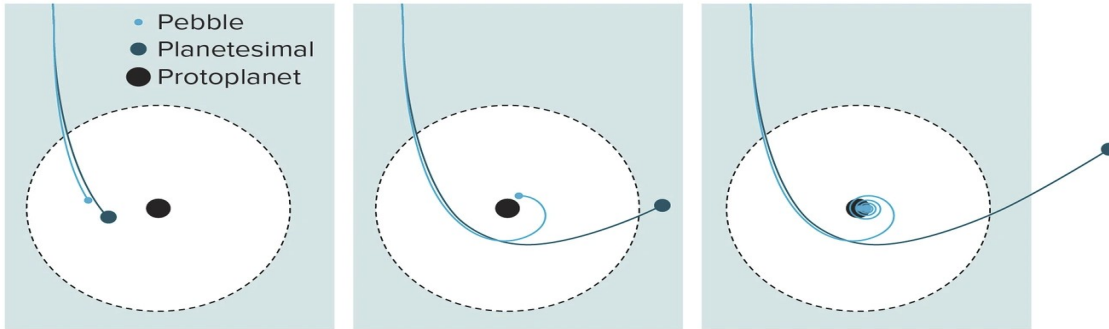
Pictorial view of the events that lead to the formation of the Moon by a giant impact.

4) Pebble accretion

Not all the dust ends up into planetesimals but, depending on the planetesimal formation process, a significant amount of mass can remain in the form of pebbles, decimeter size rocky-icy bodies. In presence of gas, they migrate inwards and can be captured by a growing embryo. Ormel and Klahr, 2010, have shown that the cross section for pebble impacts on a protoplanet is strongly enhanced by the gas drag on the pebbles. The rate of growth of protoplanets and giant planet cores can be significantly higher than in a planetesimal only scenario, leading to shorter timescale for the formation of bigger bodies.

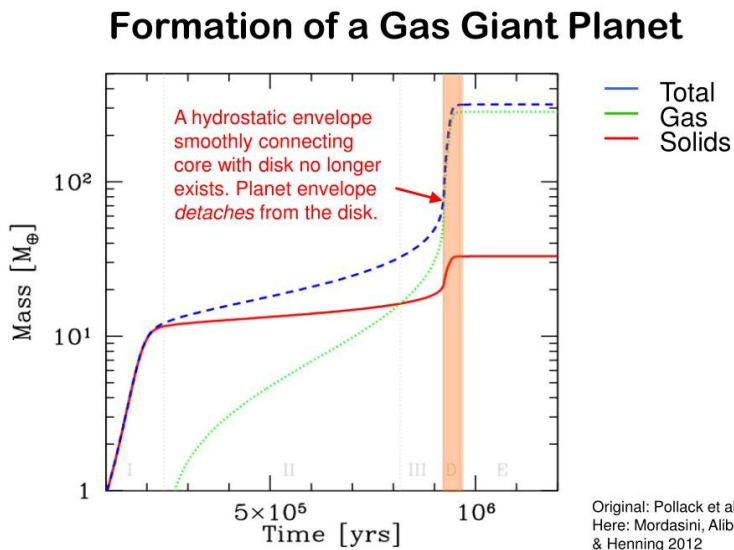
A pull on pebbles

A pebble flying past a protoplanetary body is slowed by friction from surrounding gas as it enters the protoplanet's gravitational influence (dotted line). That slowdown allows the small pebble to be captured by the protoplanet's gravity and spiral in for a smash-up, whereas a larger planetesimal just zips by. Over time, many pebbles will coalesce with the protoplanet, allowing it to grow large quickly.



Two mechanisms can halt pebble accretion 1) the dissipation of the gas of the disk which drags the pebbles towards a protoplanet and 2) if the planet carves a gap in the disk and generates pressure bumps at the edge of its orbit stopping the inward flux of pebbles.

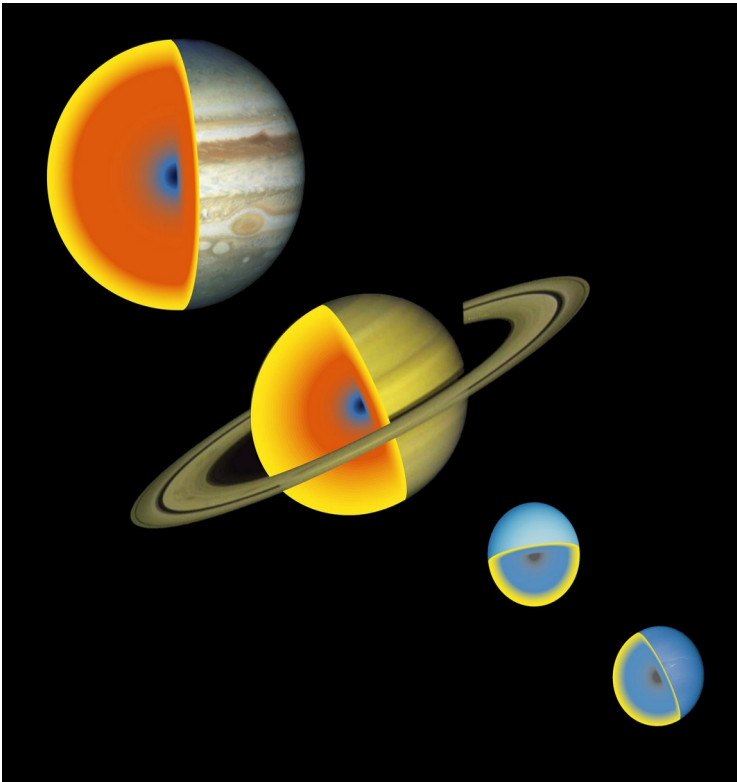
5) Gas infall onto the giant planet cores.



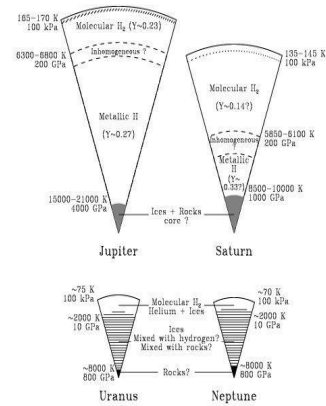
Once a protoplanet reaches a mass of a 10-30 Earth masses, a fast (~ 1000 yr) mass infall of gas onto the rocky-icy core occurs. This is shown in the figure where the growth of Jupiter vs. time is shown. The final mass of the giant planet is then reached.

Structure of the giant and icy planets.

The four outer planets of the solar system are divided in giant planets (Jupiter and Saturn) and icy planets (Uranus and Neptune). Their structure is summarized in the figure here below.



The yellow is for molecular hydrogen, red for metallic hydrogen, blue for ices and black for rock.



Hydrogen may become solid at elevated pressures and it shows metallic properties at ultrahigh pressures where electrons in the material are free to move like those in a metal. On Earth recent experiments

seem to indicate that such state is indeed achievable in laboratory (Loubeyre et al., 2020). This state might also be related to the strong magnetic field of Jupiter and Saturn. How do we know the composition of Jupiter? Via hydrostatic models based on data taken from spacecraft on the gravity and magnetic field of the planet, superficial temperature and pressure, chemical atmospheric composition, energy emission, Concerning Uranus and Neptune, progress in our understanding of these planets has been slowed by a lack of data compared to Jupiter and Saturn and by the inherent complexities of the planets themselves.

Uranus' radius is larger than Neptune's but its mass is smaller and Neptune is denser than Uranus by ~30%. Neptune's heat flux shows that it is still cooling, while Uranus is near equilibrium with solar insolation. Structure models suggest that Uranus and Neptune possess atmospheres with three main components: hydrogen, helium and methane. The interior is probably made of a rocky

core and icy mantle. The ice-to-rock fraction is 4 times the solar value for Neptune and 15 times for Uranus (Podolak and Reynolds, 1987). The figure shows the expected structure of the two planets. (Helled et al., 2011, Nettelmann et al., 2013)

